Technetium-99m-MIBI Uptake in Benign and Malignant Bone Lesions: A Comparative Study with Technetium-99m-MDP

Biray Caner, Mehmet Kitapçl, Mustafa Unlü, Günaydin Erbengi, Tamer Çalikoğlu, Talat Göğüş, Coşkun Bekdik

Departments of Nuclear Medicine and Orthopedics, Hacettepe University Medical Faculty, Ankara Oncology Hospital, Ankara, Turkey

The potential of hexakis (methoxyisobutylisonitrile) technetium (1) (MIBI) for the imaging of various bone pathologies and for assessment of effectiveness of therapy were investigated in a prospective study. MIBI was evaluated in comparison to MDP bone scans in 73 bone lesions (31 benign, 42 malignant). With MIBI, all but six malignant lesions were clearly visualized and the mean lesion/contralateral (L/C) ratio (2.21 ± 1.17) was significantly higher than that of benign counterparts (1.26 ± 0.40) ($p < 0.0005$). No such significance was detected on corresponding MDP bone scans (4.86 ± 3.48 versus 3.11 ± 1.52). Ten cases with malignant tumor underwent both pre- and post-therapy MIBI evaluation and it was demonstrated that radiotherapy and/or chemotherapy significantly inhibited MIBI uptake. Moreover, post-therapeutic MIBI uptake was a good reflection of the effectiveness of therapy as confirmed by histopathological evaluation. Thus, with a strikingly higher uptake in malignant bone lesions MIBI might have good potential for the detection of malignant bone pathologies as well as for assessing tumor response to therapy.

J Nucl Med 1992; 33:319–324

Hexakis (methoxyisobutylisonitrile) technetium (1) (MIBI) was originally introduced for myocardial perfusion studies (*1–2*). Recently, its noncardiac applications such as visualization of benign and malignant lesions in the lung (*3,4*), mediastinal and pulmonary metastasis from thyroid cancer (*5*), astrocytoma (*6*), and undifferentiated mesenchymal tumor (*7*) have been reported. MIBI has biological properties similar to ^{201}TI, which proved to be of value in evaluation of tumor viability and tumor response to therapy (*8*). It has also been reported that MIBI accumulates within the mitochondria and cytoplasma of cells on the basis of the electrical potentials generated across the membrane bilayers and that malignant tumors maintain higher (more negative) mitochondrial and plasma transmembrane potentials secondary to their increased metabolic requirements that could promote increased accumulation of MIBI in malignant tumors (*9*). Moreover, it was reported that metabolic blockade could depress MIBI cellular uptake (*10*).

With these considerations in mind, the potential of MIBI for the imaging of various bone pathologies and for assessment of effectiveness of therapy was investigated in a prospective study of 73 patients.

MATERIALS AND METHODS

Patients

A total of 73 patients (25 females and 48 males, age range: 10/12 mo–65 yr) with various bone pathologies were studied after obtaining informed consent. Forty-two had malignant bone pathologies [osteosarcoma (11), Ewing's sarcoma (18), metastatic lesions to bone (6), undifferentiated mesenchymal tumor (4), chondrosarcoma (3), while 31 patients had benign pathologies, recent traumatic bone fracture without complication (6), acute osteomyelitis (6), diabetic foot (2), osteochondroma (5), enchondroma (2), fibrous dysplasia (3), osteoid osteoma (1), Paget's disease (1), brown tumor (1), aneurysmal bone cyst (2), Sudeck's atrophy (1), and degenerative arthritis (1)].

Imaging

Thirty–sixty minutes following intravenous injection of MIBI (7.4 MBq/kg) a total-body study was performed. Spot images of pathological areas also were taken. Corresponding MDP bone images were acquired 72 hr following the MIBI study (3 hr after intravenous injection of 10.5 MBq/kg ^{99m}Tc-MDP). A gamma camera with a LEAP collimator was used for both MIBI and MDP studies.

Evaluation

Reports have set the optimum imaging time for MIBI to be between 30–60 min after injection (*3,11*). Thus, 30–60 min postinjection was used in our study. The MIBI and MDP bone images were visually evaluated by two blinded nuclear medicine physicians and concensus was then reached concerning the visualization or nonvisualization of lesions. Since visual interpretation was rather subjective, the ratios of lesion/contralateral (L/C) were also calculated on both MIBI and corresponding MDP images by placing ROIs over the lesion and contralateral normal

Received Apr. 29, 1991; revision accepted Oct. 8, 1991.
For reprints contact: Biray Caner, MD, Assoc. Professor, Bestekar Sok. 19/15 Kavaklidere 06680 Ankara, Turkey.

areas. In some cases, intense uptake of muscles was noted in the contralateral extremity. In such cases, the nearest normal area in the affected extremity was used as a reference region.

Ten patients with histopathologically proven malignant bone tumors [osteosarcoma (5), Ewing's sarcoma (4), undifferentiated mesenchymal tumor (1)] underwent both pre- and post-therapy (7–8 wk following either chemotherapy and/or radiotherapy) evaluation of both MIBI and MDP. Post-therapy biopsy was also performed to assess the therapeutic response of tumor. Histologic grading of the effect of therapy on tumor was based on the degree of cellularity and necrosis in the biopsy specimen. Grades III and IV responses (>95% and 100% necrosis, respectively), indicating extensive to complete response in the primary tumor, were considered favorable. Grades I and II responses (<50% and <50%–95%, respectively), indicating minimal destruction of the tumor, were unfavorable (*12*). Clinical improvement/worsening was determined by an oncologist for each of the ten patients relative to the changes in pain and swelling.

RESULTS

Patient data (e.g., diagnosis and L/C ratios obtained on MIBI and MDP images) are summarized in Table 1 for malignant and Table 2 for benign bone lesions. The mean L/C ratios with MIBI were 2.21 ± 1.17 for malignant and 1.26 ± 0.40 for benign lesions ($p < 0.0005$). Corresponding L/C ratios with MDP were 4.86 ± 3.48 and 3.11 ± 1.52, respectively ($p > 0.005$). Thirty-six of 42 malignant tumors (85.7%) were clearly demonstrated by MIBI, while 6 lesions [Ewing's sarcoma (5), undifferentiated adenocarcinoma metastases to sternum (1)] were not visualized as localized increased uptake on MIBI images. Figure 1 shows the distribution of MIBI L/C ratios in malignant and benign lesions.

All undifferentiated mesenchymal tumors studied (n = 4) had positive MIBI uptake, but in another patient with undifferentiated adenocarcinoma neither metastasis to the sternum nor the primary site in the lungs were visualized using MIBI.

Metastatic deposits in four cases (three with lung metastases and one with metastatic lymph nodes) were also clearly identified using MIBI, but not with MDP.

Most of the benign lesions studied (20 out of 31) (64.5%) were not visualized on MIBI images. Interestingly, none of the recent traumatic bone fractures had positive MIBI uptake. On the other hand, the remaining 11 patients (35.4%), with either acute osteomyelitis, aneurysmal bone cyst, or diabetic foot, were clearly demonstrated on MIBI images.

The L/C ratios of 10 patients who underwent both pre- and post-therapeutic evaluation with MIBI and MDP are shown on Table 3. Post-therapeutic images of both MIBI and MDP were compared to the corresponding pre-therapeutic images and then were rated as: improvement, no change and worsening. Improvement was decided if the post-therapeutic L/C ratio was at least 20% less than the corresponding pre-therapeutic value. Conversely, worsening indicated that the post-therapeutic L/C ratio was at least 20% higher than that of pre-therapeutic value. Seven of ten cases showed improvement with MIBI. These seven cases demonstrated favorable tumor response histologically (Grade III or IV). On the other hand, in the remaining three patients, no change with MIBI was detected. In two patients, unfavorable responses were demonstrated and in one favorable tumor response was demonstrated. Only three of eight cases demonstrating favorable tumor response histologically showed improvement with MDP.

TABLE 1
Clinical Findings and L/C Ratios of MDP and MIBI in Malignant Bone Pathologies

Case	Age/Sex	Diagnosis	MDP L/C ratio	MIBI L/C ratio
1*	10/12 M	Undiffer. mesenchymal	5.12	1.77
2*	33 M	Osteosarcoma	3.9	2.72
3	11 M	Metastatic adenoca.	1.7	1.41
4*†	16 M	Osteosarcoma	9.64	6.02
5	38 M	Chondrosarcoma	2.98	1.70
6	29 F	Osteosarcoma	3.9	2.66
7	15 F	Ewing's sarcoma	2.1	1.10 (N.V.)
8	39 M	Chondrosarcoma	2.06	1.59
9‡	25 M	Undiffer. mesenchymal	2.10	1.20
10	48 M	Chondrosarcoma	14.26	1.20
11	5 F	Ewing's sarcoma	6.40	1.76
12*	3 F	Ewing's sarcoma	5.40	1.18
13	47 M	Metastatic adenoca.	2.40	1.95
14	14 F	Ewing's sarcoma	2.01	1.13
15	21 M	Osteosarcoma	5.96	3.82
16*	15 M	Ewing's sarcoma	5.73	4.17
17*	8 F	Ewing's sarcoma	2.30	1.57
18	9 F	Ewing's sarcoma	3.90	1.50
19	15 F	Osteosarcoma	8.70	2.01
20	21 M	Metastatic adenoca.	2.80	2.01
21*	31 F	Osteosarcoma	3.01	2.80
22‡	21 M	Osteosarcoma	13	3.94
23	20 F	Ewing's sarcoma	3.54	1.22
24	11 M	Ewing's sarcoma	1.23	0.98 (N.V.)
25	13 M	Ewing's sarcoma	1.41	1.08 (N.V.)
26	52 F	Undiffer. mesenchymal	5.53	1.70
27	7 M	Ewing's sarcoma	1.27	1.05 (N.V.)
28*	14 F	Osteosarcoma	4.90	4.80
29	22 M	Osteosarcoma	4.90	2.91
30	60 M	Undiffer. adenocarmet.	3.10	0.90 (N.V.)
31	11 M	Ewing's sarcoma	3.80	1.06 (N.V.)
32	21 M	Ewing's sarcoma	3.60	2.25
33	21 M	Ewing's sarcoma	1.53	1.40
34‡	17 M	Ewing's sarcoma	3.43	2.50
35	65 F	Metastatic adenoca.	6.20	3.40
36	11 M	Ewing's sarcoma	4.16	2.21
37	22 M	Metastatic adenoca.	5.96	3.90
38	16 M	Ewing's sarcoma	17.68	1.60
39	23 M	Osteosarcoma	6.91	1.70
40*	17 M	Osteosarcoma	4.70	2.42
41	13 F	Undiffer. mesenchymal	6.07	2.90
42*	18 F	Ewing's sarcoma	4.65	3.43

* Patients underwent both pre- and post-therapy evaluation by both MIBI and MDP.
† Patients with metastatic lymph nodes.
‡ Patients with lung metastases. N.V. = nonvisualized.

TABLE 2
Clinical Findings and L/C Ratios of MDP and MIBI in Benign Bone Pathologies

Case	Age/Sex	Diagnosis	MDP L/C ratio	MIBI L/C Ratio
1	37 M	Osteomyelitis	2.30	1.30
2	52 M	Osteomyelitis	2.30	1.40
3	28 M	Osteomyelitis	5.10	1.80
4	15 M	Osteomyelitis	5.05	1.88
5	12 M	Osteomyelitis	3.88	1.24
6	12 M	Osteomyelitis	1.33	1.24
7	52 M	Diabetic foot	3.33	1.98
8	21 M	Osteochondroma	2.10	1.08 (N.V.)
9	18 M	Osteochondroma	1.10	0.98 (N.V.)
10	29 F	Osteochondroma	2.76	0.96 (N.V.)
11	9 F	Osteochondroma	2.28	1.50 (N.V.)
12	43 M	Enchondroma	1.20	0.96 (N.V.)
13	47 M	Enchondroma	1.50	1.01 (N.V.)
14	29 M	T. Fracture	2.00	0.99 (N.V.)
15	48 M	T. Fracture	1.50	1.01 (N.V.)
16	21 F	T. Fracture	4.45	0.98 (N.V.)
17	48 M	T. Fracture	1.50	1.01 (N.V.)
18	42 M	T. Fracture	6.98	0.98 (N.V.)
19	34 M	T. Fracture	5.54	1.05 (N.V.)
20	21 F	Osteoid osteoma	2.82	1.02 (N.V.)
21	57 F	Paget's disease	3.65	1.01 (N.V.)
22	21 F	Fibrous dysplasia	3.59	1.10 (N.V.)
23	8 F	Aneurysmal bone cyst	5.80	2.30
24	18 M	Brown tumor	1.90	0.96 (N.V.)
25	64 M	Diabetic foot	2.09	1.38
26	7 F	Aneurysmal bone cyst	4.70	1.90
27	42 F	Osteochondroma	2.10	0.97 (N.V.)
28	18 F	Fibrous dysplasia	2.98	1.01 (N.V.)
29	28 M	Fibrous dysplasia	3.92	1.04 (N.V.)
30	33 M	Sudeck's atrophy	4.20	2.21
31	52 F	Degenerative arthritis	2.60	1.01 (N.V.)

(N.V.) = nonvisualized and T. Fracture = traumatic fracture.

Figure 2 presents the comparisons of tumor response to changes in L/C ratios of MIBI/MDP studies.

In 17 cases, we noted that the extent of increased uptake on MDP bone scans was larger than that on the corresponding MIBI images. However, in three cases, increased activity seen on MIBI was clearly more extensive than that seen with MDP. For the latter, tumor involvement in three patients was detected histologically not only in bone but also in adjacent soft tissues.

Figures 3–8 are representative cases with various bone pathologies.

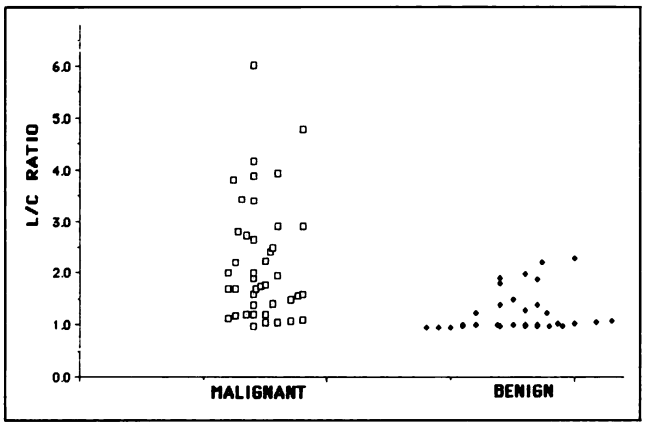

FIGURE 1. Distribution of L/C ratio in malignant and benign lesions using MIBI. (□) malignant; (■) benign.

TABLE 3
Pre- and Post-Therapeutic L/C ratios of MIBI and MDP Images: Histological and Clinical Evaluation after Therapy

Case	Pre-therapy L/C		Post-therapy L/C		Histologic grading	Clinical improvement
	MIBI	MDP	MIBI	MDP		
1	1.77	5.12	0.77	6.23	IV	Yes
2	1.57	2.30	1.30	4.71	II	±
3	2.80	3.01	1.70	3.00	III	Yes
4	2.72	3.90	1.44	3.57	III	Yes
5	6.02	9.64	1.70	1.76	III	±
6	4.17	5.73	1.01	2.31	IV	Yes
7	1.18	5.40	1.02	6.96	III	Yes
8	4.80	4.90	4.70	6.20	I	No
9	3.43	4.65	1.66	4.50	III	Yes
10	2.42	4.70	1.19	3.20	III	Yes

DISCUSSION

So far, various radiopharmaceuticals have been proposed as bone tumor imaging agents. Gallium-67 is popular, but poor physical characteristics, the necessity of long waiting periods after intravenous injection, and its lack of specificity are disadvantages. Although MDP, a nonspecific agent, can localize primary and metastatic sites of tumors in the skeletal system, it can rarely demonstrate metastatic deposits in the lung or lymph nodes. Recently, ^{201}Tl has been proposed to be a sensitive radiopharmaceutical for detection of bone sarcoma and evaluation of response to therapy (*8*). Yet its long biologic half-life limits

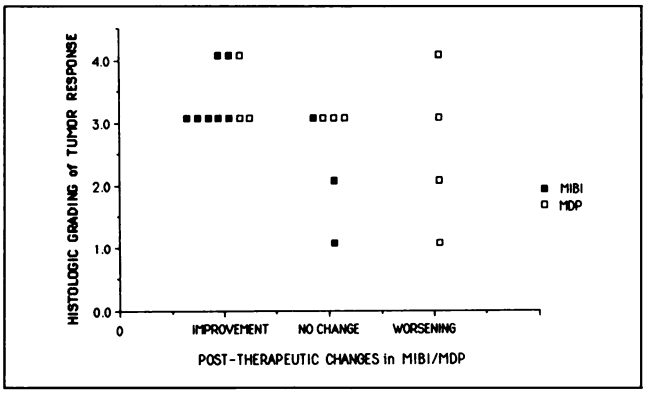

FIGURE 2. Comparison of changes in scintigraphic studies performed pre- and post-therapeutically with tumor response determined histologically. Correlation of favorable tumor response with changes in MIBI is better than that with MDP. (■) MIBI and (□) MDP studies.

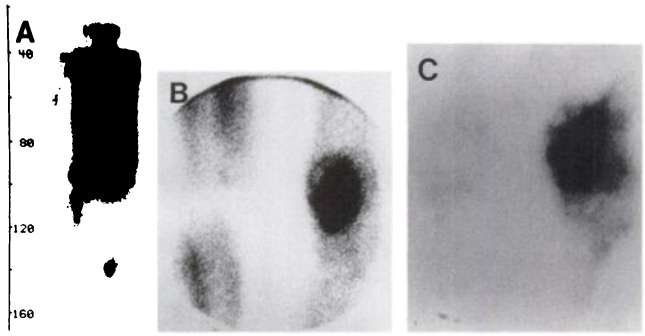

FIGURE 3. Osteogenic sarcoma of the left distal femur. MIBI images (A: whole-body, B: spot image) and the bone scan (C) show increased uptake in the tumoral region. Note that muscle activity in the unaffected extremity seems to be higher than the affected leg, probably due to overuse of it.

the administered dose, frequently resulting in long imaging times.

MIBI is a well known myocardial perfusion agent. Recently, however, its accumulation has been demonstrated in several human carcinoma cell lines in vitro (*13*). The cellular uptake mechanism of MIBI remains unresolved, but recent data indicate that distribution of MIBI in vivo is not only a simple function of blood flow, but also represents metabolic function. Pharmacological alterations in membrane transport and metabolic status can affect myocardial net accumulation and uptake kinetics (*10*).

Regardless of uptake mechanism, the results presented here suggest that MIBI, with the superiority of technetium as a radiolabel and its availability as a kit, might play an important role in the detection of both the bone tumor itself as well as the tumor's metastatic sites. Our data also demonstrated that radiotherapy and/or chemotherapy significantly inhibit the uptake of MIBI and, thus, it can be used to evaluate the effectiveness of therapy.

Thirty-six of 42 malignant lesions (85.7%) were detected by localized increased uptake of MIBI. On the other hand, only 11 of 31 benign lesions (35.48%) were visible with MIBI. The mean L/C ratio of malignant lesions was significantly higher than that of benign lesions.

Although malignant lesions tended to have higher MIBI uptake, overlap between L/C ratios for benign and malignant lesions must be kept in mind if differentiation of benign and malignant lesions is in question. We believe that MIBI uptake seems to be more closely related to other conditions such as blood flow, presence of tumor necrosis, metabolic demand and mitochondrial activity of lesions rather than lesion status (benign or malignant).

L/C ratios in malignant tumors ranged between 0.9 and 6.02. Heterogeneity of tumor blood flow, metabolism, necrosis and some other factors might cause these uptake differences. The most striking uptake was noted in cases with osteosarcoma, with a mean L/C ratio of 3.25 ± 1.28. It was significantly higher than the mean L/C ratio of other malignant bone tumors ($p < 0.0005$).

The intensity of uptake in Ewing's sarcoma was quite variable and ranged from 0.98 to 4.17. The reason for such varying degrees of uptake remains unknown. Recent work suggests that an osseous equivalent of a malignant, small-cell neoplasm of neural crest origin apparently exists within the bones (Askin tumor) and its differentiation from Ewing's sarcoma is difficult (*14*). The tumors diagnosed as Ewing's sarcoma that were not visualized on the MIBI images might be such newly described tumors originating from the neural crest. A detailed histopathological evaluation is needed to understand the reason for differences in uptake.

MIBI uptake appears unrelated to the degree of differentiation of the tumor since four patients with undifferentiated mesenchymal tumor showed positive MIBI uptake, while in another case with undifferentiated adenocarcinoma of the lung, neither the primary site in the lung

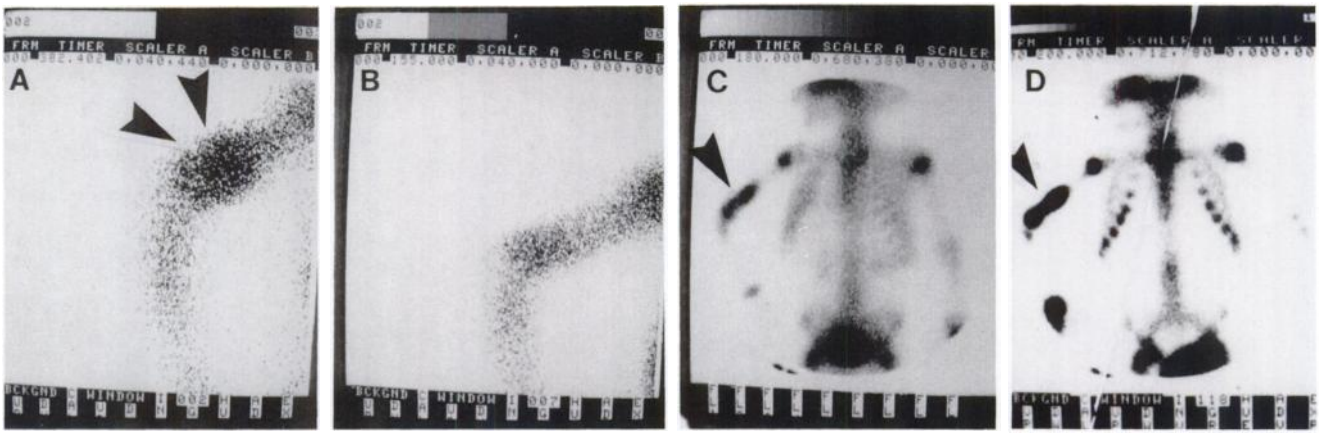

FIGURE 4. Malignant mesenchymal tumor of the right distal humerus. Pre-therapeutic MIBI image of the right arm (A) shows increased uptake in the tumoral region (arrowheads). Following radiotherapy (2000 cGy) and chemotherapy (Vincristine, Epirubicine, Cyclophosphamide), a post-therapeutic MIBI scan (B) was performed and successfully demonstrated the effectiveness of therapy as confirmed by histological evaluation. No significant change in tumoral activity between pre-therapeutic and post-therapeutic MDP bone scans (C and D, respectively) is seen (arrowhead).

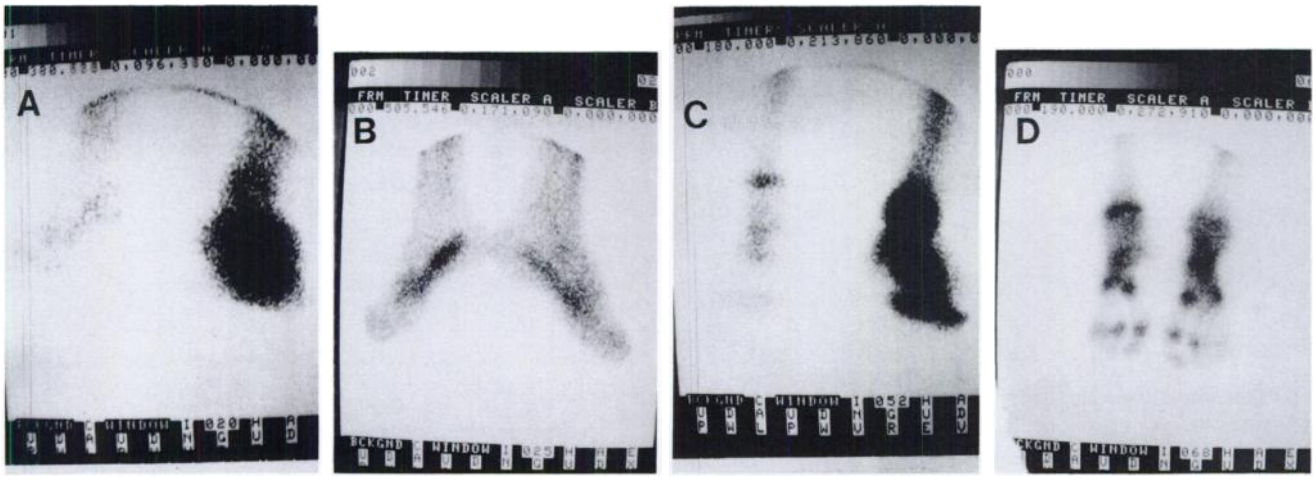

FIGURE 5. Comparison of pre- and post-therapeutic MIBI images of a patient with Ewing's sarcoma of the left foot. Intense uptake with a L/C ratio of 4.17 is seen on the MIBI image taken prior to therapy (A), while significant reduction in activity suggesting regression of tumor is noted on post-therapy MIBI image (B). L/C ratio on latter image was calculated as 1.01 and this improvement was concordant with favorable tumor response (Grade IV). Post-therapy MDP images (D) also showed improvement compared to pre-therapy image (C).

nor the metastases to the sternum were visualized on MIBI images.

In most of the cases, we noted that the extent of the pathology seen on MDP images was generally larger than that on the corresponding MIBI images. This was thought to be due to the assumption that MDP uptake is a reflection of both bone blood flow and osteoblastic activity (*15*). The extensive uptake pattern seen with MIBI, when compared to a MDP bone scan, may be explained by the fact that MIBI accumulates in both the bone and also the soft-tissue component of the tumor. In all three patients with extensive uptake pattern with MIBI, the soft-tissue component of the tumor in addition to bone involvement was detected histologically.

It was reported that in the post-therapeutic stage bone scans are not ideal for evaluating tumor response to chemotherapy, since the scans reflect a healing response as well (*16*). In two of our cases demonstrating favorable tumor response histologically, "worsening", indicating a flare phenomenon, was detected with MDP, whereas, seven of eight cases with favorable tumor response showed improvement with MIBI. Detailed studies with different chemotherapeutic regimens as well as follow-up studies will be required to determine the potential of MIBI to predict the effectiveness of therapy.

It might be difficult to evaluate MIBI uptake in tumors located at the pelvic bones or vertebrae, since MIBI activity in the gastrointestinal area might obscure the underlying

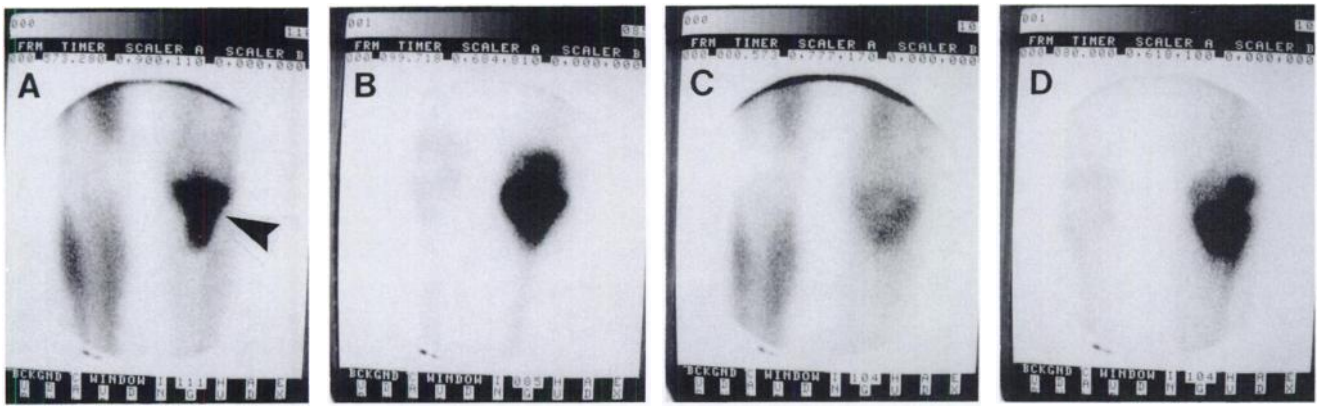

FIGURE 6. Assessment of tumor response to therapy in a patient with osteogenic osteosarcoma of proximal left tibia (arrowhead). Pre-therapeutic MIBI (A) and MDP (B) images show increased radioactivity in the diseased area (L/C ratio of MIBI: 2.72, L/C ratio of MDP: 3.90). The extended pattern seen on MDP does not exist with MIBI. The effectiveness of therapy is clearly demonstrated on the post-therapeutic MIBI image (C) as a low grade of increased activity compared to the pre-therapeutic image (L/C: 1.44). The necrotic area supporting the effectiveness of therapy is also seen. Post-therapy MDP image (D) with L/C ratio of 3.57 showed no significant change compared to corresponding pre-therapy image.

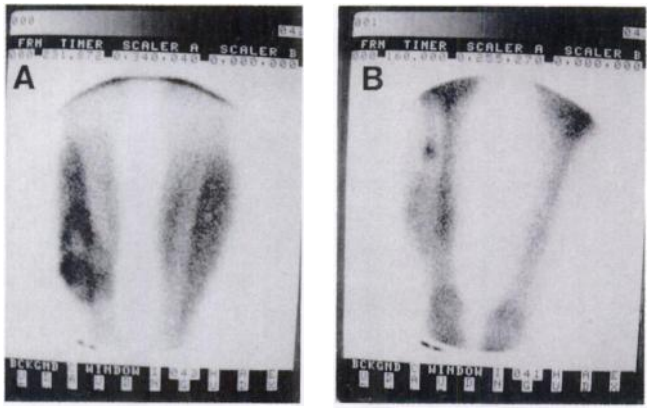

FIGURE 7. Recurrent osteosarcoma of right fibula of a young male. Partial fibulectomy, radiotherapy and chemotherapy was performed a year before admission. On admission, a large fixed mass with a hyperemic skin on the surface was palpated at the mid-lateral portion of right calf. Anterior MIBI image (A) shows a high uptake in the tumoral region. The intensity of uptake on the corresponding MDP image (B) is lower than that seen on the MIBI image. It was thought that MDP accumulation is primarily limited to bone, whereas MIBI accumulates in both bone and soft-tissue components of tumor.

abnormality. Prominent cardiac uptake might also cause difficulties in evaluating certain intrathoracic tumors. These difficulties might be solved by the use of SPECT.

We believe that the MDP bone scan as the basic screening method cannot be replaced by MIBI bone imaging. However, MIBI imaging might provide additional information to that obtained by the MDP bone scan at presentation and during follow-up of patients. At presentation, the extent of tumor and lung or lymph node metastases can be demonstrated with MIBI. In the follow-up period, MIBI also might provide useful information regarding assessment of response to treatment and local recurrence.

In conclusion, this study demonstrates the utility of MIBI to identify malignant lesions of bone and to assess tumor response to therapy.

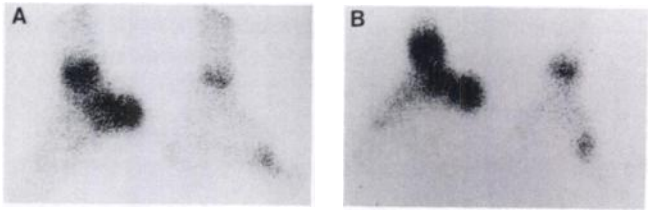

FIGURE 8. Acute osteomyelitis of the right foot. Both MIBI (A) and MDP (B) images show obvious intense uptake in the affected region.

REFERENCES

1. Watson, Smith WH, Teates CD, et al. Quantitative myocardial imaging with Tc-99-MIBI. Comparison with Tl-201 [Abstract]. *J Nucl Med* 1987; 28:653.
2. Baillet GY, Mena IG, Kuperus JH, et al. Simultaneous technetium-99m-MIBI angiography and myocardial perfusion imaging. *J Nucl Med* 1989; 20:38–44.
3. Hassan IM, Sahweil A, Constantinides C, et al. Uptake and kinetics of Tc-99m hexakis 2-methoxy isobutyl isonitrile in benign and malignant lesions in the lungs. *Clin Nucl Med* 1989;14:333–340.
4. Muller SP, Reiner C, Paas M, et al. Tc-99m-MIBI and Tl-201 uptake in bronchial carcinoma [Abstract]. *J Nucl Med* 1989;30:845.
5. Muller ST, Guth-Tougelides B, Creutzig H. Imaging of malignant tumors with Tc-99m-MIBI SPECT [Abstract]. *J Nucl Med* 1987;30:845.
6. O'Tuama LA, Packard AB, Treves ST. SPECT imaging of pediatric brain tumor with hexakis (methoxyisobutylisonitrile) technetium (1). *J Nucl Med* 1990;31:2040–2041.
7. Caner B, Kitapçi M, Erbengi G, et al. Increased accumulation of Tc-99m-MIBI in undifferentiated mesenchymal tumor and its metastatic lung lesions. *Clin Nucl Med* 1991:in press.
8. Ramanna L, Waxman A, Binney G, et al. Thallium-201 scintigraphy in bone sarcoma: comparison with gallium-67 and technetium-MDP in the evaluation of chemotherapeutic response. *J Nucl Med* 1990;31:567–572.
9. Chiu M, Kronauge JF, Piwnica-Worms D. Effect of mitochondrial and plasma-membrane potentials on accumulation of hexakis (2-methoxyisobutylisonitrile) technetium (1) in cultured mouse fibroblasts. *J Nucl Med* 1990;31:1646–1653.
10. Piwnica-Worms D, Kronauge JF, Delmon L, et al. Effect of metabolic inhibition on technetium-99m-MIBI kinetics in cultured chick myocardial cells. *J Nucl Med* 1990;31:464–472.
11. Caner B, Kitapçi M, Aras T, et al. Increased accumulation of hexakis [2-methoxyisobutylisonitrile technetium (1)] in osteosarcoma and its metastatic lymph nodes. *J Nucl Med* 1991;32:1977–1978.
12. Makawer MM, Link MP, Donaldsan SS. Sarcomas of bone. In: De Vita VT, Hemlan S, Rosenberg SA, eds. *Cancer principles and practice of oncology*, third edition. Philadelphia: J.B. Lippincott; 1989:1418–1442.
13. Delmon-Moingeon LI, Piwnica-Worms D, Van den Abbeele AD, et al. Uptake of the cation hexakis (2-methoxyisobutylisonitrile) technetium-99m by human carcinoma cell lines in vitro. *Cancer Res* 1990;50:2198–2202.
14. Mirra JM. Neurogenous tumors, In: Mirra JM, ed. *Bone tumors: clinical, radiological, and pathological correlations.* Philadelphia; London: Lea and Febiger; 1989:849–855.
15. Chew FS, Hudson TM. Radionuclide bone scanning of osteosarcoma: falsely extended uptake pattern. *AJR* 1982;139:49–54.
16. Pollen JJ, Witztum KF, Asburn WL. The flare phenomenon on radionuclide bone scan in metastatic prostate cancer. *AJR* 1984;142:773–776.